Journal of Hazardous Materials 188 (2011) 319–333

Contents lists available at ScienceDirect

Journal of Hazardous Materials

journal homepage: www.elsevier.com/locate/jhazmat

Modeling and evaluation of chromium remediation from water using low cost bio-char, a green adsorbent

Dinesh Mohan[a,*], Shalini Rajput[a], Vinod K. Singh[a], Philip H. Steele[b], Charles U. Pittman Jr.[c]

[a] School of Environmental Sciences, Jawaharlal Nehru University, New Delhi 110067, India
[b] Forest Products Department, Mississippi State University, Mississippi State, MS 39762, USA
[c] Department of Chemistry, Mississippi State University, Mississippi State, MS 39762, USA

ARTICLE INFO

Article history:
Received 14 October 2010
Received in revised form 27 January 2011
Accepted 27 January 2011
Available online 4 February 2011

Keywords:
Bio-char
Low cost adsorbent
Chromium
Hexavalent chromium
Chromium removal
Chromium adsorption

ABSTRACT

Oak wood and oak bark chars were obtained from fast pyrolysis in an auger reactor at 400–450 °C. These chars were characterized and utilized for Cr(VI) remediation from water. Batch sorption studies were performed at different temperatures, pH values and solid to liquid ratios. Maximum chromium was removed at pH 2.0. A kinetic study yielded an optimum equilibrium time of 48 h with an adsorbent dose of 10 g/L. Sorption studies were conducted over a concentration range of 1–100 mg/L. Cr(VI) removal increased with an increase in temperature ($Q^{\circ}_{\text{Oak wood}}$: 25 °C = 3.03 mg/g; 35 °C = 4.08 mg/g; 45 °C = 4.93 mg/g and $Q^{\circ}_{\text{Oak bark}}$: 25 °C = 4.62 mg/g; 35 °C = 7.43 mg/g; 45 °C = 7.51 mg/g). More chromium was removed with oak bark than oak wood. The char performances were evaluated using the Freundlich, Langmuir, Redlich–Peterson, Toth, Radke and Sips adsorption isotherm models. The Sips adsorption isotherm model best fits the experimental data [high regression (R^2) coefficients]. The overall kinetic data was satisfactorily explained by a pseudo second order rate expression. Water penetrated into the char walls exposing Cr(VI) to additional adsorption sites that were not on the surfaces of dry char pores. It is remarkable that oak chars (S_{BET}: 1–3 $m^2\ g^{-1}$) can remove similar amounts of Cr(VI) as activated carbon (S_{BET}: ~1000 $m^2\ g^{-1}$). Thus, byproduct chars from bio-oil production might be used as inexpensive adsorbents for water purification. Char samples were successfully used for chromium remediation from contaminated surface water with dissolved interfering ions.

1. Introduction

Chromium is the earth's 21st most abundant element (about 122 ppm) and the sixth most abundant transition metal [1]. The principal chromium ore is ferric chromite ($FeCr_2O_4$). Other sources include crocoite, $PbCrO_4$, and chrome ochre, Cr_2O_3. Chromium occurs in 2+, 3+ and 6+ oxidation states but Cr^{2+} is unstable and very little is known about its hydrolysis [1–3]. The hydrolysis of Cr(III) is complicated. It produces mononuclear species $CrOH^{2+}$, $Cr(OH)_2^{+}$, $Cr(OH)_4^{-}$, neutral species $Cr(OH)_3^{0}$ and polynuclear species $Cr_2(OH)_2$ and $Cr_3(OH)_4^{5+}$ [4]. The hydrolysis of Cr^{6+} produces only neutral and anionic species, predominately CrO_4^{2-}, $HCrO_4^{2-}$, $Cr_2O_7^{2-}$ [2,1]. At low pH and high chromium concentrations, $Cr_2O_7^{2-}$ predominates while at a pH greater than 6.5, Cr(IV) exists in the form of CrO_4^{2-} [1,2]. Trivalent chromium is a hard acid and forms relatively strong complexes with oxygen and donor ligands. Chromium(VI) compounds are of more concern than Cr(III) due to their high water solubility and mobility [1,5]. The most soluble, mobile and toxic forms of Cr(VI) in soils are chromate and dichromate. Hexavalent chromium is rapidly reduced to trivalent chromium under aerobic conditions [5].

Acute exposure to Cr(VI) causes nausea, diarrhea, liver and kidney damage, dermatitis, internal hemorrhaging, and respiratory problems [3]. Inhalation may cause acute toxicity, irritation and ulceration of the nasal septum and respiratory sensitization (asthma) [1–3,5,6]. Skin contact may result in systemic poisoning or severe burns, and interference with the healing of cuts or scrapes. If not treated promptly, this may lead to ulceration and severe chronic allergic contact dermatitis. Eye exposure may cause permanent damage.

Chromium is both beneficial and detrimental. Chromium(III) is an essential trace element in mammalian metabolism. In addition to insulin, it is responsible for reducing blood glucose levels, and is used to control certain cases of diabetes [7]. It has also been found to reduce blood cholesterol levels by diminishing the concentration of (bad) low density lipoproteins "LDLs" in the blood [7]. Cr(III) is supplied in a variety of foods such as Brewer's yeast, liver, cheese, whole grain breads and cereals, and broccoli [1].

Chromium compounds are widely used in electroplating, metal finishing, magnetic tapes, pigments, leather tanning, wood protection, chemical manufacturing, brass, electrical and electronic equipment, catalysis and so on [1]. Leather is the 5th largest export

* Corresponding author. Tel.: +91 11 6704616; fax: +91 11 26704616.
E-mail address: dm_1967@hotmail.com (D. Mohan).

0304-3894/$ – see front matter © 2011 Elsevier B.V. All rights reserved.
doi:10.1016/j.jhazmat.2011.01.127

from India, a leading leather manufacturing countries. Tanning is a major consumer of water, most of which is discharged as waste. The volume and characteristics of different wastewater streams from a tannery depend on the processes adopted for water consumption, which vary from tannery to tannery. In Kanpur, India, a cluster of more than 60 tanneries are situated on the bank of the Ganga River. Kanpur is one of India's most severely polluted cities. Its eastern districts feature about 350 industrial leather tanneries, many of which discharge untreated waste into local groundwater sources and the Ganges River. These tanneries process hides into leather employing chrome and vegetable tanning. The wastewaters from these units are the main cause of chromium contamination in Kanpur. Very high chromium concentrations, on the order of 16.3 mg/L (16,300 μg/L), were found in these waters versus the permissible concentrations of 0.05 mg/L (50 μg/L) recommended for drinking water [8]. High concentrations within this area's sediments were reported [8]. The drinking water guideline for total chromium recommended by the US Environmental Protection Agency (EPA) is 100 μg/L [9]. According to Bureau of Indian Standards (BIS), the permissible and desirable chromium limits in drinking water is 0.05 mg/L [10]. Such chromium ground water contamination emphasized the need to develop low cost technology suitable to apply under local conditions.

Treatment technologies to remove chromium from water include chemical precipitation [11], constructed wetland [12], ion exchange [13,14], membrane separation [15], ultrafiltration [16], sedimentation [17], adsorption [1,18], etc. Chemical precipitation has traditionally been used the most. Frequently used precipitation processes include precipitation with hydroxide, sulfide, carbonate and phosphate. The precipitation of chromium hydroxide is induced by the addition of a base, but this method produces sludge. It changes the aqueous pollution problem to a solid waste disposal problem without recovering the metal. Ion exchange is considered a better alternative, but it has high operational costs. Most remediation methods remove chromium more effectively from water containing relatively high initial chromium concentrations (usually above 100 mg/L). Adsorption has evolved as the front line of defense for chromium removal. Selective adsorption by red mud [19], coal [20], photocatalyst beads [21], nano-particles [22,23], fertilizer industrial waste [24], biomass [25], activated sludge biomass [26], etc. has generated increasing excitement.

Low cost adsorbents used in chromium remediation from water and wastewater have been reviewed by Mohan and Pittman [1]. Biosorbents used for chromium removal were reviewed by Saha and Orvig [27]. Different adsorbents used for metal ion removal were also discussed [28,29]. For several years we have tried developing low cost adsorbents/activated carbons for the removal and recovery of toxic metals, including tri-and hexavalent chromium, from water [2,3,30–34]. Sorption properties of bio-chars have been explored for the remediation of organic and inorganic contaminants from water [35–37]. Recently, we have successfully applied byproduct bio-chars, generated during bio-oil production, for the remediation of metals from water [37]. In a continuation of our earlier work [37], we demonstrate the successful use of bio-chars for remediating hexavalent chromium from water.

2. Reagents and equipment

All chemicals were AR-grade. The stock solution of chromium(VI) was prepared by dissolving $K_2Cr_2O_7$ in doubly distilled water. The pH measurements were made using a pH meter (Model EUTECH, pH 510). Test solution pHs were adjusted using H_2SO_4 (0.1N) and NaOH (0.1 N). The aqueous total chromium concentrations in the samples were determined by atomic absorption spectrophotometer model Thermo Scientific M Series with an air-acetylene flame and chromium hollow cathode lamp. Adsorbent–adsorbate agitation was carried out on a water bath shaker (model RC51000). Mettler Toledo balance (model AB 265-S/FACT) was used for measuring the weights. The Cr(VI) concentrations in surface water were measured using a UV–vis spectrophotometer model PerkinElmer Lammda 35 at 540 nm after developing color by adding diphenyl carbazide. The light metals in surface water were measured using a Flame photometer model CL-378, Elico, India. Conductivity, TDS and ORP were determined using a multi-parameter ion meter model Thermo Orion 5 Star.

The oak wood and oak bark chars were characterized by infrared spectroscopy, gas adsorption (N_2, −196 °C), mercury density (ρ_{Hg}), helium density (ρ_{He}) and specific surface area (S_{BET}) as described in detail previously [37].

The specific surface area (S_{BET}) was evaluated from the N_2 adsorption isotherms by applying the Brunauer et al. equation [38] in the relative pressure (p/p^0) range between 0.05 and 0.35, and taking a_m (i.e., the average area occupied by a molecule of N_2 in the completed monolayer) to be equal to 16.2 Å^2. Also, the micro- and mesopore volumes (V_{mi}, V_{me}) were obtained from the adsorption isotherms. V_{mi} was taken as the volume of N_2 adsorbed (V_{ad}) at $p/p^0 = 0.10$ and V_{me} as the volume of N_2 adsorbed (V_{ad}) at $p/p^0 = 0.95$ minus the V_{ad} at $p/p^0 = 0.10$. The micropore volume (W_0) was further estimated by applying the Dubinin–Radushkevich equation [39,40], as given by Eq. (1):

$$\log W = \log W_o - D \log^2(p^0/p) \quad (1)$$

where W is the micropore volume that has been filled with liquid N_2 when the relative pressure is p/p^0 and W_0 is the total micropore volume. D is a characteristic constant of the micropore structure of the adsorbent. V_{mi}, V_{me}, and W_0 were expressed as liquid volumes. The total pore volume (V_T) was calculated by making use of expression:

$$V_T = \frac{1}{\rho_{Hg}} - \frac{1}{\rho_{He}} \quad (2)$$

Char constituents were analyzed by standard chemical methods [37,41,42].

The morphological structure of the oak wood char and oak bark char were obtained using a scanning electron micrograph (Zeiss, EVO 40). In the SEM analysis, the samples were coated with a thin layer of gold and mounted on a copper stab using a double stick carbon tape.

3. Pyrolysis of oak wood and oak bark and adsorbent development

Bio-chars were produced by pyrolyzing oak wood and oak bark in an auger reactor as reported earlier [37]. The oak bark samples were air dried for 1–2 days to 8–10% moisture content. Oak wood samples were used as received (6–8% moisture) [37]. Each feed was ground and sieved to a particle size of 2–6 mm before pyrolysis. Two treatments (at 400 and 450 °C) were employed for each pyrolysis feed. The wood or bark chars pyrolyzed at these two temperatures were mixed together before use in adsorption studies. Chars were used directly without any grinding or chemical treatment to reduce the cost [37].

4. Time–temperature profile for wood/bark pyrolysis

The time–temperature pyrolysis profile in the auger pyrolysis reactor for the wood/bark was discussed thoroughly in our earlier publication [37]. We refer the reader to this paper for the exact description of the reactor and pyrolysis process. The char traversed the reactor at 36 in./min. The total time spent in the two pyrolytic

zones was ~30 s with an additional ~13–14 s in the heated zone 3 [37].

Chars were sieved (>600, 600–250, 250–177, 177–149, and <149 μm) and the particle size fraction from 600 to 250 μm was used without modification throughout the study unless otherwise stated.

5. Sorption procedure

Batch sorption studies were carried out to obtain rate and equilibrium data. Different temperatures and adsorbent doses were employed to obtain equilibrium isotherms and the data required for design and operation of fixed-bed reactors to treat chromium contaminated water.

5.1. Sorption studies

The effect of pH was observed by studying the Cr(VI) adsorption over a broad pH range of 2–10. In the equilibrium studies both solution pH and temperature were adjusted. A known amount (10 g/L) of bio-char (particle size 600–250 μm) was added to each flask followed by agitation for specified times to a maximum of 48 h. The contact time and conditions were selected based on preliminary experiments. These demonstrated that equilibrium was established in 48 h. No further uptake occurred between 48 and 72 h. After this period, solutions were filtered using Whatman filter paper No. 1 and analyzed by atomic absorption spectrometry for the Cr(VI) concentration remaining in the solution. The sorption studies were also carried out at three temperatures, viz, 25, 35 and 45 °C, to determine the effect of temperature and to evaluate the sorption thermodynamic parameters.

Amount of chromium removed/adsorbed was determined using the following mass balance equation:

$$q_e = \frac{(c_0 - c_e)V}{W} \quad (3)$$

where q_e is the amount (mg/g) of chromium adsorbed, c_0 and c_e are the initial and equilibrium chromium concentrations (mg/L) in solution, V is the adsorbate volume (L), and W is the adsorbent weight (g).

5.2. Sorption dynamics

Large-scale adsorption processes for water treatment demand inexpensive, nontoxic, locally available adsorbents of known kinetic parameters and sorption characteristics. Once optimal conditions are determined, process design and modeling can easily be done. Thus, the effects of contact time, adsorbent dose and concentrations were investigated. At desired temperatures, predetermined amounts of char were added to stoppered flasks having 50-mL chromium solutions in a thermostatic shaking assembly. The solutions were agitated. At predetermined intervals char was separated and the solutions were analyzed for chromium. The chromium adsorbed was calculated by Eq. (3). Similar studies were carried out at different chromium concentrations keeping adsorbent dose and temperature constant for bio-chars.

5.3. Quality assurance/quality control

All batch isotherm tests were replicated twice and the experimental blanks were run in parallel to establish accuracy, reliability and reproducibility. All glassware was presoaked in a 5% HNO_3 solution, rinsed with double distilled water and oven-dried. Blanks were run and corrections applied if necessary.

Table 1
Properties of bio-chars generated from oak wood and oak bark at 400 and 450 °C and then blended [37].

Properties of char	Oak wood char	Oak bark char
Proximate[a]		
Moisture (%)	3.17(0.00)	1.56(0.00)
Ash (%)	2.92(3.02)	11.09(11.27)
Volatile (%)	15.58(16.09)	22.82(23.18)
Fixed carbon (%)	78.33(80.89)	64.53(65.55)
Higher heating value, HHV (kJ/kg)	31059(32076)	25774(26181)
Low heating value, LHV (kJ/kg)	30470(31468)	25202(25600)
Ultimate[a]		
C (%)	82.83(85.54)	71.25(72.38)
H (%)	2.70(2.78)	2.63(2.67)
N (%)	0.31(0.32)	0.46(0.47)
S (%)	0.02(0.02)	0.02(0.02)
O[b](%)	8.05(8.32)	12.99(13.19)

[a] Values in parenthesis are for dry char and without parenthesis are for as received char.
[b] By difference.

6. Results and discussion

6.1. Characterization

Chars were sieved >600, 600–250, 250–177, 177–149, and <149 μm and the particle size fraction from 600 to 250 μm was used without modification throughout the study unless otherwise stated.

The infrared spectra of these adsorbents have been discussed earlier [37]. Bands due to different oxygen-containing surface groups (C=O, C–O, –OH) and others (olefins, $–CH_2$, CH_3, aromatic rings) were observed. Since lignocellulosic samples were charred at relatively low temperatures, only partial aromatization occurred [37]. The proximate and ultimate analyzes of oak wood and oak bark are given in Table 1 [37]. The "ultimate analysis" gives the charred biomass composition in wt% of carbon, hydrogen and oxygen as well as sulfur and nitrogen (if any). Proximate analysis gives the chars' fixed carbon, volatile and ash contents. Elemental carbon, hydrogen and nitrogen analysis of the bio-oil samples was conducted by combustion. Oxygen was determined by difference. Percent ash, moisture, fixed carbon, and higher heating value (HHV) are also given in Table 1.

Chars were ashed to determine the inorganic constituents. The ash was dissolved totally in HF and analyzed by plasma emission spectroscopy. The chemical constituents (dry weight% basis) of these ashed chars are summarized in Table 2.

Oak bark char has a higher calcium content than oak wood char. Furthermore, oak wood char has a higher carbon content than oak bark char. The calorific value of char was measured as HHV. The lower heating value (LHV) was calculated from the HHV and the total weight percent of hydrogen in the char (from elemental anal-

Table 2
Elemental analysis of oak wood and oak bark chars [37].

Chemical constituents	Values (%)	
	Oak wood char	Oak bark char
Al_2O_3	0.76	0.39
BaO	0.45	0.28
CaO	68.0	92
Fe_2O_3	1.40	0.21
K_2O	3.43	0.53
MgO	5.20	1.18
MnO	2.70	1.51
Na_2O	1.63	0.31
SiO_2	5.82	2.66
SrO	0.35	0.49
TiO_2	0.06	0.02

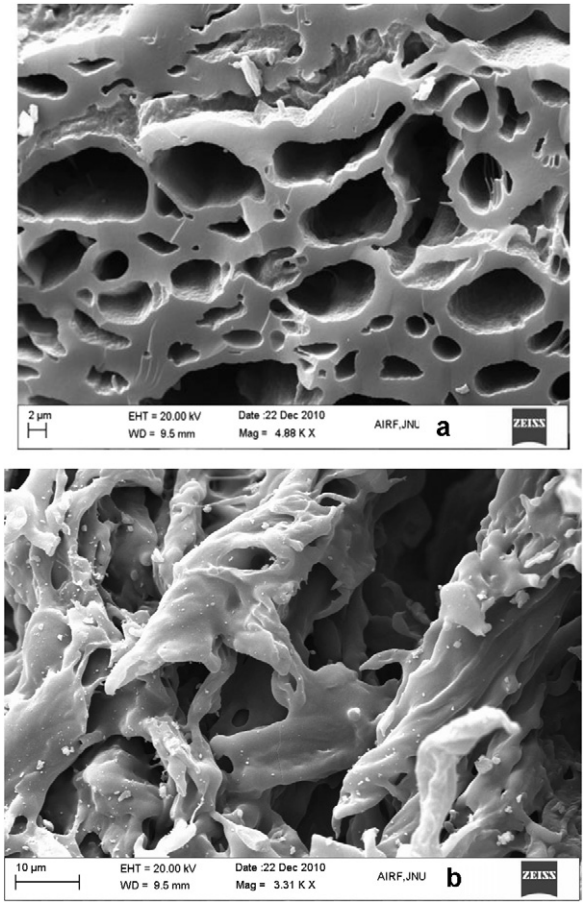

Fig. 1. SEM photographs of oak bark bio-char at different magnifications. (a) 4.88k× and (b) 3.31k×.

ysis) by Eq. (4).

$$\text{LHV}\ \ [\text{J/g}] = \text{HHV}\ \ [\text{J/g}] - 218.13 \times H\%\ \ [\text{wt\%}] \quad (4)$$

Oak wood chars had higher HHV values than oak bark chars. Char samples were stirred with deionized water (5 g/L) at an initial pH 7.10 for 2 h and left for 24 h in an airtight-stoppered flask. The pH value decreases slightly.

The nitrogen adsorption isotherms for the oak bio chars were discussed earlier [37]. All the isotherms exhibited a hysteresis loop, characteristic of Type IV isotherms. These isotherms are typical for mesoporous solids [43]. If materials contain mesopores (i.e., pore widths between 20 and 500 Å) and micropores (with additional external surface area), the isotherms display an initial ascending branch up to $p/p^0 \sim 0.20$. Next, these isotherms show a rather straight portion, which extends up to $p/p^0 = 0.60–0.80$. This positive plateau slope (in the relative pressure range 0.2–0.8) indicates that mesopore development has started. Finally, there is an upward sweep near the saturation pressure. The increase in the N_2 adsorption at high p/p^0 values is greater for activated carbon. The values of S_{BET}, V_{mi}, V_{me}, W_0, and V_T are listed in Table 3.

Morphological analysis was performed by scanning electron microscopy. SEM micrographs (Figs. 1 and 2) clearly show the amorphous and heterogeneous nature of oak wood and oak bark chars. Scanning electron spectroscopy images revealed that mesopores are present in bio-char materials. These pores are of importance to many liquid–solid adsorption processes. The bio-char surface and sub-surface chemistry contains a rich variety of oxygen-containing functional groups including hydroxy, anhydride, carboxylic acid, ketone, quinoid, ether, hydroxyl ketone and

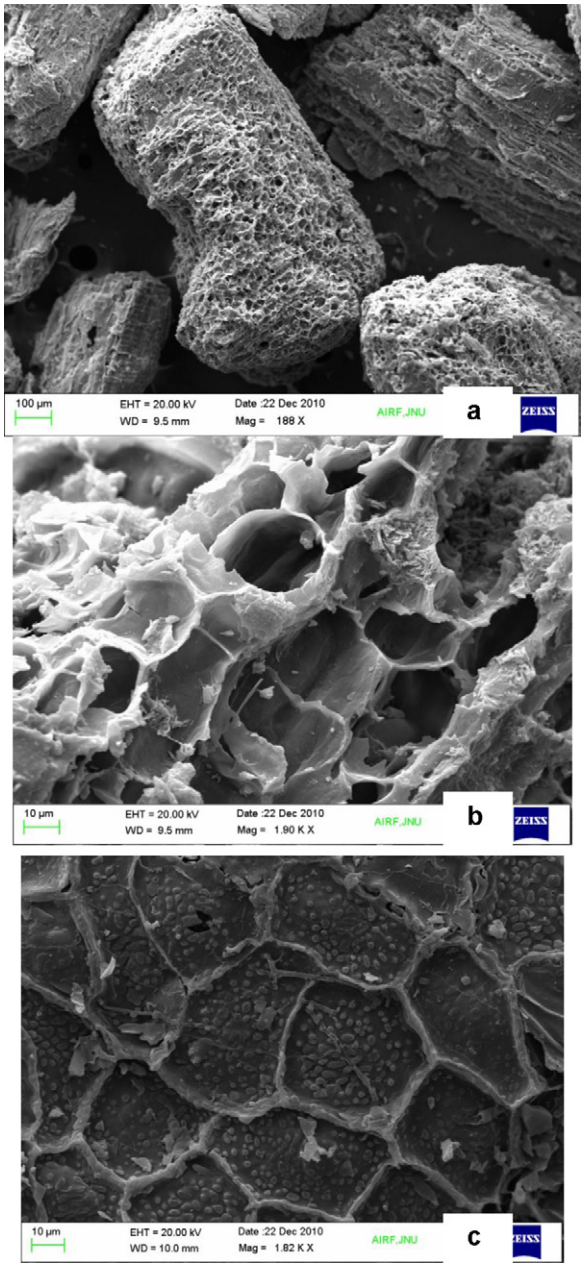

Fig. 2. SEM photographs of oak wood bio-char at different magnifications. (a) 188×, (b) 1.90k× and (c) 1.82k×.

other functions. They contain hydrophilic and hydrophobic sites and provide both acidic and basic sites. The relative contributions of these functional groups and properties depend upon both the feedstock and on the thermal decomposition process variables (time, temperature, heat transfer rates, particle size distribution, reactor configuration, etc.) [44].

Fig. 1a shows the predominant oak bark char morphology, while the micrograph. Fig. 1b shows a region which may have been exposed to high temperature longer or it initially may have had a local bark chemical composition that appeared to distort on pyrolysis to a semi-melt. Oak wood char particles are shown in Fig. 2a. Fig. 2b zooms in on a particle showing the predominant morphology closer up. The micrograph (Fig. 2c) shows a section of less predominant morphology. These SEM micrographs show that residual wood porosity and morphology remains in the char (it looks like a somewhat distorted picture of a cut through wood itself). Obviously, the short heating time of the

Table 3
Textural data and density values for oak wood and oak bark chars [37].

Char samples	[a] S_{BET} ($m^2\ g^{-1}$)	[a,b] V_{mi} ($cm^3\ g^{-1}$)	[a] W_O ($cm^3\ g^{-1}$)	[a,b] V_{me} ($cm^3\ g^{-1}$)	[a] ρ_{Hg} ($g\ cm^{-3}$)	[a] ρ_{He} ($g\ cm^{-3}$)	[a,b] V_T ($cm^3\ g^{-1}$)
Oak wood	2.73	9.1×10^{-4}	7.381×10^{-4}	1.64×10^{-3}	0.91	1.45	0.41
Oak bark	1.88	6.6×10^{-4}	6.575×10^{-4}	2.94×10^{-3}	0.57	1.43	1.06

[a] (S_{BET}: BET specific surface area; V_{mi} and W_0: micropore volumes; V_{me}: mesopore volume; V_T: total pore volume; ρ_{Hg}: mercury density; ρ_{He}: helium density).
[b] (N_2 adsorption isotherms: $V_{mi} = V_{ad}$ at $p/p^0 = 0.1$, $V_{me} = V_{ad}$ at $p/p^0 = 0.95 - V_{ad}$ at $p/p^0 = 0.1$, $V_T = 1/\rho_{Hg} - 1/\rho_{He}$)

fast pyrolysis process has not totally destroyed the original wood cell morphological structure originally present. Instead, chemical decomposition has occurred with loss of water and organic fragments which reduces the total mass by at least 80% (assumes a 20% maximum char yield). The remaining ~20% mass is more highly carbonized than before pyrolysis but it still has 6–10% oxygen still present and maintains some of the wood or bark initial morphology.

6.2. Sorption studies

Experiments were conducted to determine the optimum pH in the range of 2–10 for chromium removal by oak wood and oak bark chars (Fig. 1). Initial concentrations of 10 mg/L were used. The chromium removal efficiency decreased as pH increased from 2 to 10. Maximum adsorption occurs at pH 2.0. Above pH 2.0, an increase in pH causes the sharp decrease in chromium removal efficiency. The effect of pH on chromium adsorption is attributed to interactions between Cr-ions in solution and complexes formed at the adsorbent surface and within the char walls. That aqueous Cr(VI) can form a variety of species in solution at various pH's is well known in literature [1].

Cr(VI) removal as a function of pH and the equilibrium pH are presented in Fig. 3. These studies were carried out with an initial concentration of 10 mg/L. The adsorption of Cr(VI) on these bio-chars decreases with increasing pH_{in}. Fig. 1 shows that the bio-chars are active in the acidic range and especially in the low pH range. The maximum adsorption of Cr(VI) species on bio-chars adsorbents was at pH 2.0 and negligible at pH values >8. Cr(VI) can exist in several stable forms such as CrO_4^{2-}, $HCrO_4^{2-}$, $Cr_2O_7^{2-}$, and $HCr_2O_7^-$, and the relative abundance of a particular complex depends on the chromium ion concentration and the pH. The bio-char is positively charged at low pH due to surface group protonation. In contrast, the sorbates' dichromate ions are negative, leading to an electrostatic attraction between the bio-chars and sorbate. This results in increased adsorption at low pH. As the pH increases, the sorbent undergoes deprotonation, and the adsorption capacity decreases. Therefore, all subsequent studies were carried out at pH 2.0 [2]. Similar observations were reported earlier on different adsorbents [45,46].

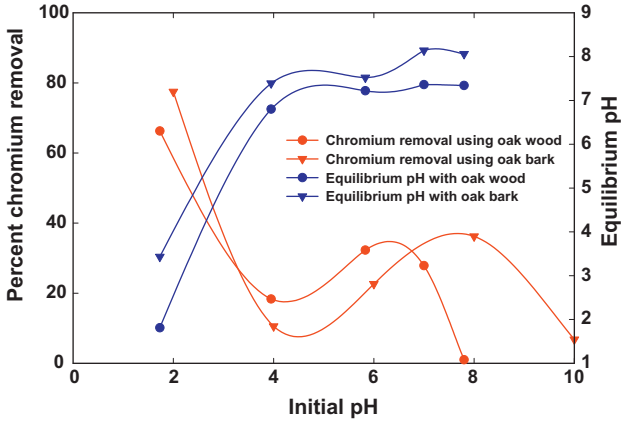

Fig. 3. Effect of pH on chromium removal using oak wood and oak bark. Chars at an initial chromium concentration of 10 mg/L, adsorbent dose of 10 g/L and at 25 °C.

Furthermore, Park et al. [47], reported that Cr(VI) removal occurred partly through reduction, as well as anionic adsorption. This reduction could only have taken place under strongly acidic conditions (pH < 2.5). According to Park et al. [47] it has been proven that Cr(VI) is easily or spontaneously reduced to Cr(III) when Cr(VI) comes in contact with organic substances or reducing agents, especially in acidic medium. Thus, reduction of Cr(VI) to Cr(III) is dependent on various factors including the nature of the adsorbent, the chromium concentration and the equilibrium time. In some cases, adsorption occurs completely through reduction, whereas in other cases, it is partially anionic and partially reduction.

When wood is subjected to fast pyrolysis, the resulting char contains substantial (8–12%) oxygen. Byproducts of lignin pyrolysis include catechol and substituted catechol. Such structures must be present in the char and they act as reducing agents while being oxidized to ortho-quinone structural units. These units are also chelating toward metal cations. Cellulose and hemicelluloses also provide unsaturated anhydrosugars, diols and other compounds which can reduce Cr(VI). Thus, these pyrolytic chars readily reduce and bind to chromium cations. A representative catechol reduction of Cr(IV) with subsequent chelation of Cr(IV) to the ortho-quinone that forms is shown in Scheme 1.

6.2.1. Kinetic studies and modeling

The effect of adsorbent quantity on the rate of chromium uptake was studied. For the comparative evaluation and to avoid the handling of large adsorbent amounts in laboratory scale batch studies, a 10 g/L bio-char was selected for all the sorption and kinetic studies. Preliminary investigations on the rate of chromium uptake on bio-chars indicated that the process is rapid. Typically 30–40% of the total adsorption occurs within the 2 h of contact (Figs. 2–6). This subsequently gives way to a very slow approach to equilibrium. In 48 h, saturation is reached.

Kinetic studies were carried out at 25, 35, and 45 °C to determine the effect of temperature. Sorption dynamics at different temperatures are presented in Figs. 2 and 4. Chromium removal on oak wood and oak bark increased with temperature, indicating the process is endothermic. Kinetics at chromium concentrations of 20, 40, 60 and 80 mg/L at 25 °C are presented in Figs. 3 and 5. An increase in the initial chromium concentration enhances the sorption rate.

In order to elucidate the adsorption mechanism, the pseudo first-order and pseudo second order kinetic models were tested to fit the experimental data obtained from batch experiments.

6.2.1.1. Pseudo first order kinetic model. A simple kinetic model that describes the process of adsorption is the pseudo-first order equation as suggested by Lagergren [48] and further cited by Ho et al. [49] and us [37]

$$q_t = q_e\,(1 - e_1^{-kt})\,(\text{non linear form}) \quad (5)$$

Scheme 1.

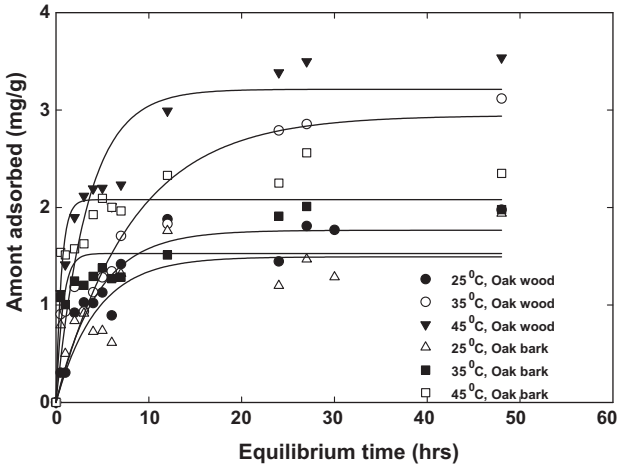

Fig. 4. Pseudo-first order kinetic plots for hexavalent chromium adsorption by oak wood and oak bark at pH 2.0 and at different temperatures: [adsorbent concentrations = 10 g/L and chromium concentration of 40 g/L].

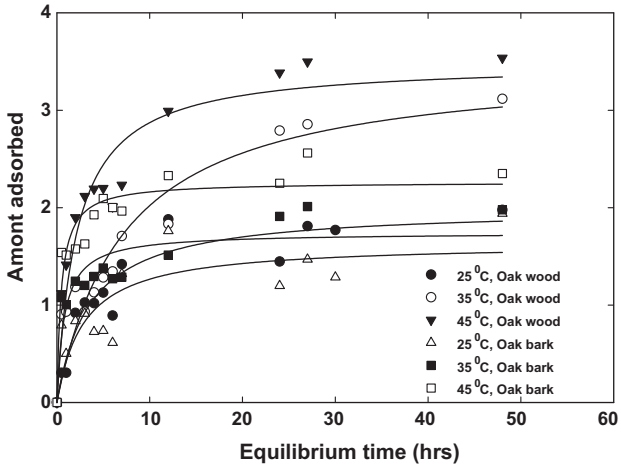

Fig. 6. Pseudo-second order kinetic plots for hexavalent chromium adsorption by oak wood and oak bark chars at pH 2.0 and at different temperatures: [adsorbent concentrations = 10 g/L and chromium concentration of 40 g/L].

where k_1 (min^{-1}) is the first order rate constant of adsorption, q_e is the chromium amount adsorbed at equilibrium and q_t is the chromium amount adsorbed at time "t."

In most cases, the Lagergren's first order equation did not apply throughout the complete range of contact time (Figs. 4 and 5). The plots were used to determine k_1 (first order rate constant) and equilibrium capacity (q_e). The values of rate constant, k_1 and regression coefficients are provided in Table 4. The regression coefficients are not very good; therefore chromium-char adsorbent systems do not follow a first-order rate equation and higher order rate equations should be applied to check their applicability. Also, the q_e values calculated from the kinetic plots are lower or higher than the experimental values at different concentrations further corroborating the above findings.

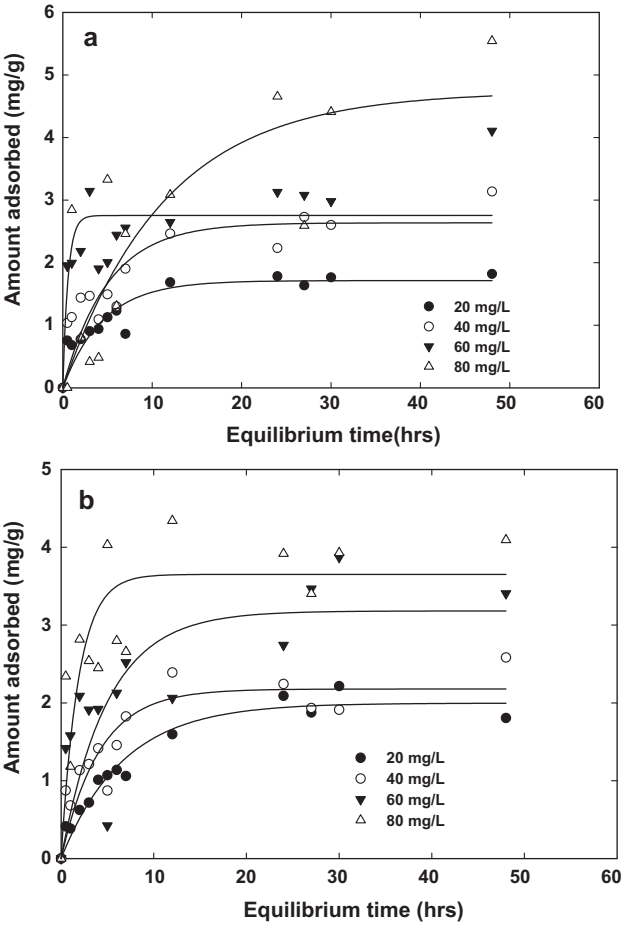

Fig. 5. Pseudo-first order kinetic plots for hexavalent chromium adsorption by (a) oak wood and (b) oak bark chars at pH 2.0 and at different chromium concentrations [adsorbent concentrations = 10 g/L and at 25 °C].

6.2.1.2. Pseudo second order kinetic model. Reactions involving pseudo-second-order processes are greatly influenced by the adsorbate amount on the adsorbent's surface and adsorbate amount adsorbed at equilibrium. This means that reaction rate is directly proportional to the number of active sites on the adsorbent's surface.

The rate expression for the pseudo-second order reaction can be written as [50]

$$\frac{d(S)_t}{dt} = k[(S)_0 - (S)_t]^2 \quad (6)$$

where $(S)_0$ and $(S)_t$ are the initial number of active sites on the adsorbent at time $t = 0$ and "t", respectively. This can be written in the form of Eq. (7) in terms of adsorbed quantity.

$$\frac{dq_t}{dt} = k_2(q_e - q_t)^2 \quad (7)$$

where k_2 ($g\,mg^{-1}\,min^{-1}$) is the pseudo second-order adsorption rate constant, q_e is the amount adsorbed at equilibrium and q_t is the amount of chromium adsorbed at time "t."

Separating the variables and then integrating leads to Eq. (8), taking into consideration that $q_0 = 0$ when $t = 0$ and that $q_t = q_t$ when $t = t$

$$\frac{1}{(q_e - q_t)^2} = \frac{1}{q_e} + k_2 t \quad (8)$$

Re-arranging Eq. (8) gives Eq. (9)

$$\frac{t}{q_t} = \frac{1}{k_2 {q_e}^2} + \frac{t}{q_e} \quad (9)$$

The product $k_2 q_e^2$ represents the initial sorption rate represented as

$$\text{Rate} = k_2 q_e^2 \quad (10)$$

The second order sorption rate constant (k_2) and q_e values were determined from the plots at different temperatures and concentrations (Figs. 6 and 7). The values of R^2 and k_2 are presented in

Table 4
First order rate constants at different temperatures and at different chromium concentration.

	Oak wood char		Oak bark char	
	First order rate constant, k_1 (h^{-1})	R^2	First order rate constant, k_1 (h^{-1})	R^2
At different temperature (°C)				
25	1.77	0.9029	1.49	0.6072
35	2.95	0.8530	1.53	0.6819
45	3.21	0.2930	2.08	0.8048
At different concentrations (mg/L)				
20	1.71	0.800	2.00	0.9520
40	2.64	0.7481	2.18	0.7931
60	2.75	0.6382	3.18	0.5030
80	4.73	0.6663	3.65	0.6960

Table 5
Second order rate constants at different temperatures and at different chromium concentrations.

	Oak wood char		Oak bark char	
	Second order rate constant, k_2 ($g\,mg^{-1}\,h^{-1}$)	R^2	Second order rate constant, k_2 ($g\,mg^{-1}\,h^{-1}$)	R^2
At different temperature (°C)				
25	2.00	0.9151	1.63	0.6542
35	3.49	0.8829	1.74	0.8071
45	3.49	0.9125	2.26	0.8986
At different concentrations (mg/L)				
20	1.87	0.8510	2.34	0.9505
40	2.91	0.8111	2.39	0.8241
60	3.00	0.7172	3.37	0.5934
80	6.12	0.6808	3.92	0.7615

Table 5. These correlation coefficients (R^2) are superior. The experimental and theoretically calculated q_e values are presented in Table 6 at different temperatures and concentrations. The theoretical q_e values are in agreement with the experimental q_e value. This suggests that the sorption system is not a first-order reaction and that a pseudo-second order model can be considered. Analysis of the regression coefficients showed that pseudo second order rate equation described the kinetic data well for both the bio-chars (Fig. 8). The pseudo-second order model is based on the assumption that the rate-limiting step may be a chemical sorption involving valance forces through sharing or exchange of electrons between adsorbent and adsorbate [51]. It provides the best correlation of the data.

6.2.2. Sorption studies and modeling

Sorption equilibrium studies at different temperatures (25, 35, 45 °C) were conducted by batch technique. The isotherms (data points) for chromium adsorption at optimum pH (2.0) on oak wood and oak bark chars are shown at three different temperatures (Figs. 9 and 10). The isotherms are positive, regular, and concave to the concentration axis. In both the cases, the chromium uptake increases with decrease in temperature confirming the process is endothermic. Optimization of chromium removal by oak wood and oak bark chars requires the most appropriate correlation to describe the adsorption equilibrium isotherms. The basic, most widely used adsorption isotherm models in liquid phase adsorption are those of Freundlich, Langmuir, Redlich–Peterson, Toth, Sips, and Radke. The performance of these chars at different temperatures was evaluated using the Freundlich, Langmuir, Redlich–Peterson, Toth, Sips, and Radke, adsorption models.

All the model parameters were evaluated using nonlinear regression employing the Sigma Plot 8.0 software.

6.2.2.1. Freundlich isotherm model. The Freundlich model does not indicate a finite uptake capacity of the sorbent. Thus, it can only reasonably apply in the low to intermediate concentration range. The nonlinear Freundlich equation [52] may be written as

$$q_e = K_F C_e^{1/n} \quad (11)$$

where q_e is the amount of chromium adsorbed per unit weight of adsorbent (mg/g), C_e is the equilibrium concentration of chromium in the bulk solution (mg/L), K_F is the constant indicative of the relative adsorption capacity of the adsorbent (mg/g) and $1/n$ is the constant indicative of the intensity of the adsorption. The nonlinear Freundlich adsorption isotherms are given in Fig. 9a and b while the parameters are reported in Table 7.

Table 6
Comparative evaluation of q_e as calculated experimentally and by using first and second order rate equations at different chromium concentrations.

Concentrations/temperatures	q_e experimental (mg/g)		q_e calculated using first order kinetic model(mg/g)		q_e calculated using second order kinetic model(mg/g)	
	Oak wood	Oak bark	Oak wood	Oak bark	Oak wood	Oak bark
Temperature						
25 °C	1.97	1.93	1.77	1.49	2.00	1.63
35 °C	3.11	1.97	2.94	1.53	3.49	1.74
45 °C	3.54	2.34	3.21	2.08	3.49	2.26
Concentrations						
20 mg/L	1.82	1.80	1.71	2.00	1.87	2.34
40 mg/L	2.60	2.58	2.62	2.17	2.91	2.39
60 mg/L	4.10	3.40	2.75	3.18	3.00	3.37
80 mg/L	5.50	4.09	4.73	3.65	6.12	3.92

Table 7
Freundlich, Langmuir, Redlich–Peterson, Toth, Sips and Radke and Prausnitz isotherm parameters for chromium removal on oak wood and oak bark chars at different temperatures.

Isotherm parameters	Oak wood char			Oak bark char		
	25 °C	35 °C	45 °C	25 °C	35 °C	45 °C
Freundlich						
K_F (mg/g)	0.436	1.095	1.038	0.523	0.942	1.332
$1/n$	0.404	0.278	0.332	0.496	0.511	0.432
R^2	0.6591	0.5854	0.6766	0.9149	0.7809	0.6534
Langmuir						
Q^0 (mg/g)	3.031	4.076	4.930	4.619	7.433	7.515
b	0.051	0.082	0.068	0.073	0.010	0.149
R^2	0.6460	0.5767	0.6658	0.9672	0.8183	0.7475
Redlich–Peterson						
K_{RP} (L/g)	0.465	3.326	4.068	0.307	0.691	0.876
a_{RP}(L/mg)$^{\beta_{RP}}$	0.687	2.771	3.606	0.045	0.066	0.024
β_{RP}	0.678	0.740	0.685	1.093	1.091	1.430
R^2	0.6568	0.5849	0.6846	0.9683	0.8190	0.7758
Toth Isotherm						
K_T (L/g)	16.92	10.08	14.81	3.972	6.250	6.008
B_T(L/mg)$^{\beta_T}$	0.180	0.757	0.306	0.070	0.099	0.125
β_T	4.375	3.642	3.586	0.6823	0.6457	0.0194
R^2	0.6563	0.5824	0.6728	0.9703	0.8211	0.8004
Sips						
K_{LF} (L/g)	0.274	0.788	0.641	0.182	$4.230\text{x}10^{-7}$	0.156
a_{LF}(L/mg)$^{a_{LF}}$	-0.560	-0.390	-0.524	0.048	$7.85\text{x}10^{-8}$	0.026
n_{LF}	0.094	0.116	0.093	1.461	13.81	3.150
R^2	**0.6668**	**0.5872**	**0.6798**	**0.9764**	**0.8853**	**0.8318**
Radke and Prausnitz						
a	49947.1	6876124.3	4265757.8	4361272.5	1697380.5	11188436.6
b	0.436	1.095	1.037	0.523	0.942	1.332
β	0.405	0.278	0.332	0.496	0.511	0.433
R^2	0.6591	0.5854	0.3317	0.9149	0.7809	0.6534

Bold letters represent the highest R^2 values.

6.2.2.2. Langmuir isotherm model. The Langmuir adsorption isotherm sheds no light on the mechanistic aspects of adsorption; it provides information on uptake capabilities and also reflects the usual equilibrium process behaviors. The nonlinear Langmuir equation [53] may be written as

$$q_e = \frac{Q^0 b C_e}{1 + bC_e} \tag{12}$$

where q_e is the amount of chromium adsorbed per unit weight of adsorbent (mg/g), C_e is the equilibrium concentration of chromium in the bulk solution (mg/L), Q^0 is the monolayer adsorption capacity (mg/g) and b is the constant. Basically it is the reciprocal value of the concentration at which half the saturation of the adsorbent is reached.

The nonlinear Langmuir adsorption isotherms are given in Fig. 10a and b while the parameters are reported in Table 7.

The essential characteristic of a Langmuir isotherm can be expressed in terms of a dimensionless constant separation factor, R_L, originally defined by Hall et al. [54] and applied by many groups. R_L factor defined by the following equation:

$$R_L = \frac{1}{1 + bC_0} \tag{13}$$

where b is the Langmuir constant; C_0 is the initial concentration and R_L indicates the shape of the isotherm ($R_L > 1$ unfavorable; $R_L = 1$ linear; $0 < R < 1$ favorable and $R_L = 0$ irreversible). The dimensionless separation factor, R_L was determined at different temperatures over a broad concentration range. The values of R_L versus temperature were found to be between 0 and 1 indicating the favorable chromium adsorption on oak wood and oak bark chars (data omitted for brevity).

6.2.2.3. Redlich–Peterson model. The Redlich–Peterson equation [55] incorporates three parameters where the exponent β, lies between 0 and 1.

$$q_e = \frac{K_{RP} C_e}{1 + a_{RP} C_e \beta} \tag{14}$$

where K_{RP}, a_{RP} and β are Redlich–Peterson constants and the exponent, β, lies between 0 and 1.

For $\beta = 1$, it reduces to Langmuir adsorption isotherm.

$$q_e = \frac{K_{RP} C_e}{1 + a_{RP} C_e} \tag{15}$$

when $\beta = 0$, it becomes Henry's equation.

$$q_e = \frac{K_{RP} C_e}{1 + a_{RP}} \tag{16}$$

The nonlinear Redlich–Peterson adsorption isotherms are given in Fig. 11a and b. The adsorption isotherm parameters and regression coefficients (R^2) are given in Table 7.

6.2.2.4. Toth isotherm model. The Toth isotherm equation is originally derived from potential theory and is applicable to heterogeneous adsorption. It assumes a quasi-Gaussian energy distribution. Most sites have an adsorption energy lower than the maximum adsorption energy [56]:

$$q_e = \frac{K_T C_e}{(1 + BC_e \beta)^{1/\beta}} \tag{17}$$

where K_T, B and β are the Toth constants.

The nonlinear Toth adsorption isotherms are given in Fig. 12a and b. The adsorption isotherm parameters and regression coefficients (R^2) are available in Table 7.

6.2.2.5. Radke and Prausnitz isotherm model. A slightly different isotherm equation with three adjustable parameters was developed by Radke and Prausnitz [57] utilizing thermodynamics

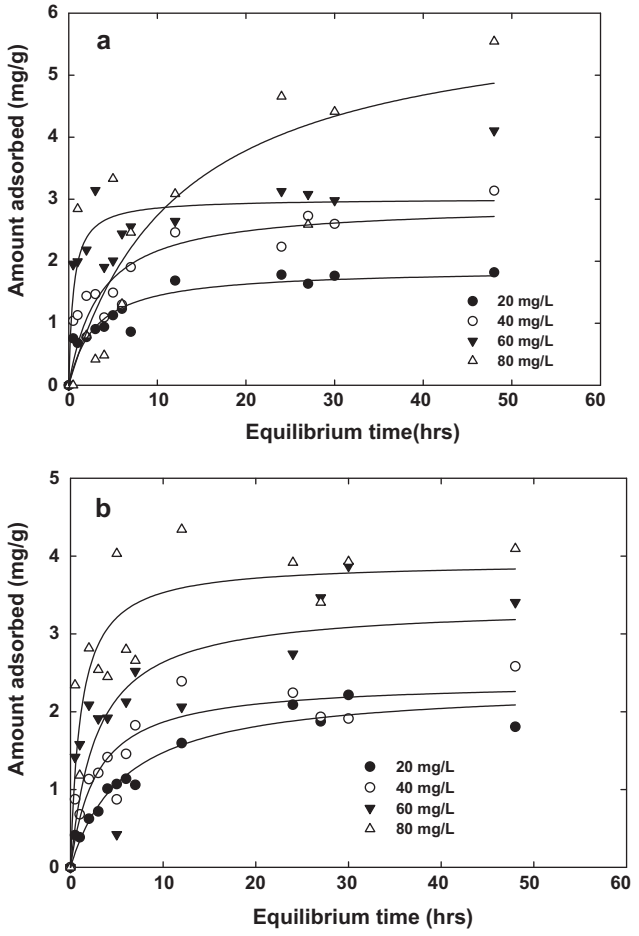

Fig. 7. Pseudo-second order kinetic plots for hexavalent chromium adsorption by (a) oak wood and (b) oak bark at pH 2.0 and at different chromium concentrations [adsorbent concentrations 10 g/L and at 25 °C].

consideration. This isotherm equation is valid for a wide range of concentrations.

$$q_e = \frac{abC_e{}^{\beta}}{a + bC_e{}^{\beta-1}} \tag{18}$$

where a, b and β are the isotherm constants for the Radke and Prausnitz isotherm model.

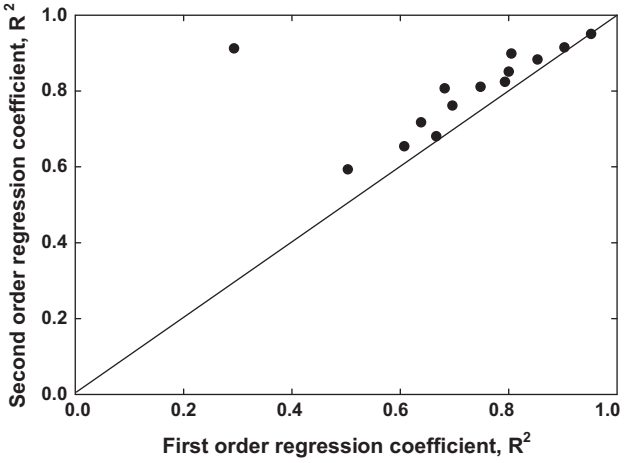

Fig. 8. Comparative evaluation of pseudo first order and pseudo second order regression coefficients obtained for hexavalent chromium adsorption by oak wood and oak bark chars.

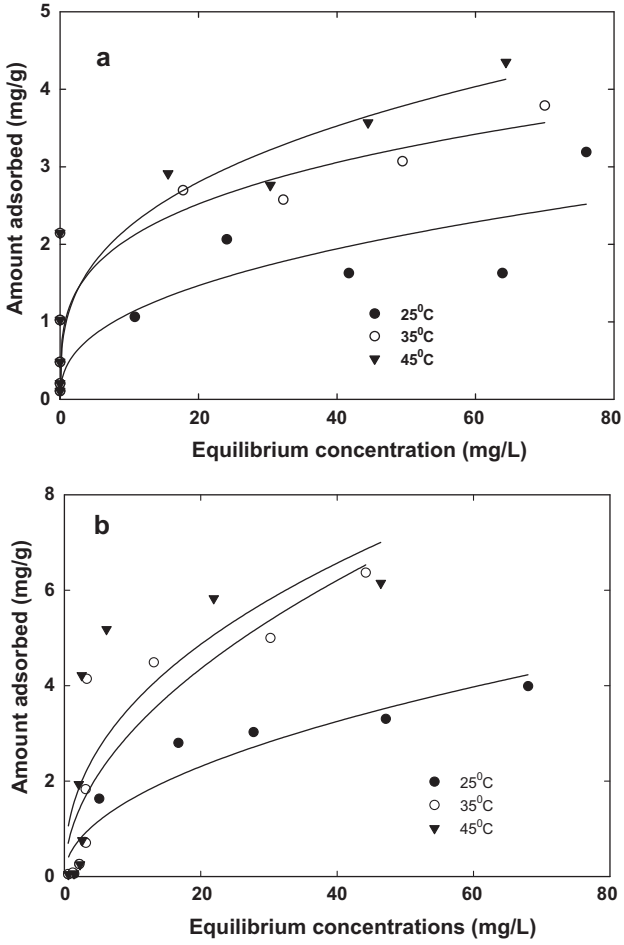

Fig. 9. Freundlich adsorption isotherms of hexavalent chromium by (a) oak wood and (b) oak bark chars at different temperatures [pH 2.0, adsorbent concentration of 10 g/L]. Solid lines represent the data fitted by the Freundlich isotherm model.

The nonlinear Radke and Prausnitz adsorption isotherms are given in Fig. 13a and b. The adsorption isotherm parameters and regression coefficients (R^2) are reported in Table 7.

6.2.2.6. Sips or Langmuir–Freundlich adsorption isotherm model. This model is a combination of Langmuir and Freundlich models. The Langmuir Freundlich or Sips [58] name derives from the limiting behavior of the equation. Although at low concentrations it does not reduce to the linear equation, at very high concentrations it predicts the surface saturation. Furthermore, at moderate concentrations, the surface heterogeneity is taken into account by the power function of concentration.

$$q_e = \frac{K_{LF}C_e{}^{n_{LF}}}{1 + (a_{LF}C_e)^{n_{LF}}} \tag{19}$$

where K_{LF}, a_{LF} and n_{LF} are the sips constants.

The nonlinear Sips or Langmuir–Freundlich adsorption isotherms are given in Fig. 14a and b while the adsorption isotherm parameters and regression coefficients are reported in Table 7.

The Langmuir model fits the data better than the Freundlich model. The Langmuir model is used to estimate maximum uptake values, where these could not be obtained experimentally. The constant "*b*" represents the affinity of the bio-chars and chromium.

Among all the isotherm models applied to fit the data, the Sips or Langmuir–Freundlich adsorption isotherm model best fits the experimental data with high regression (R^2) coefficients which are shown in bold in Table 7. This means that adsorption of chromium

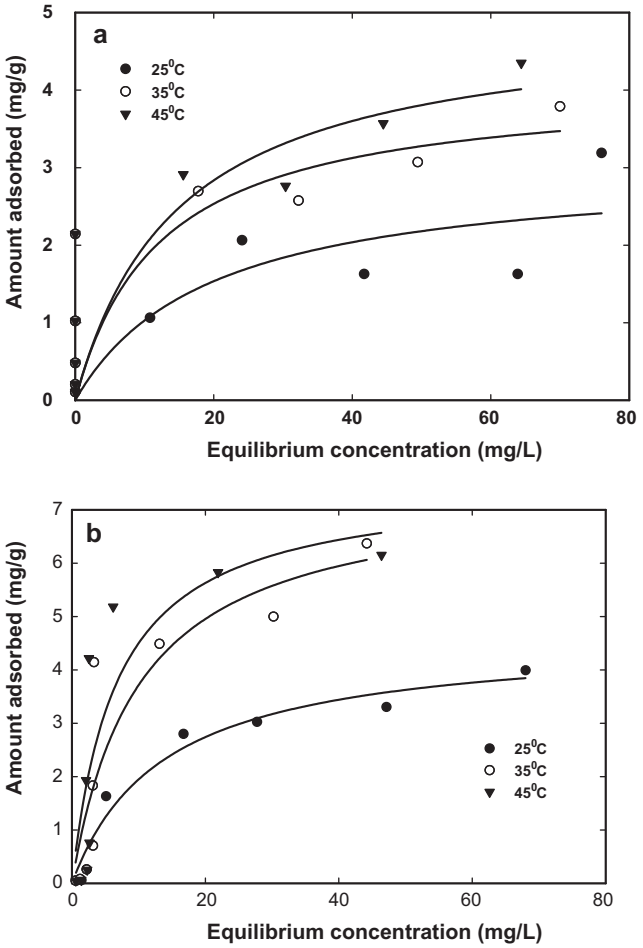

Fig. 10. Langmuir adsorption isotherms of hexavalent chromium by (a) oak wood and (b) oak bark chars at different temperatures [pH 2.0, adsorbent concentration of 10 g/L]. Solid lines represent the data fitted by the Langmuir isotherm model.

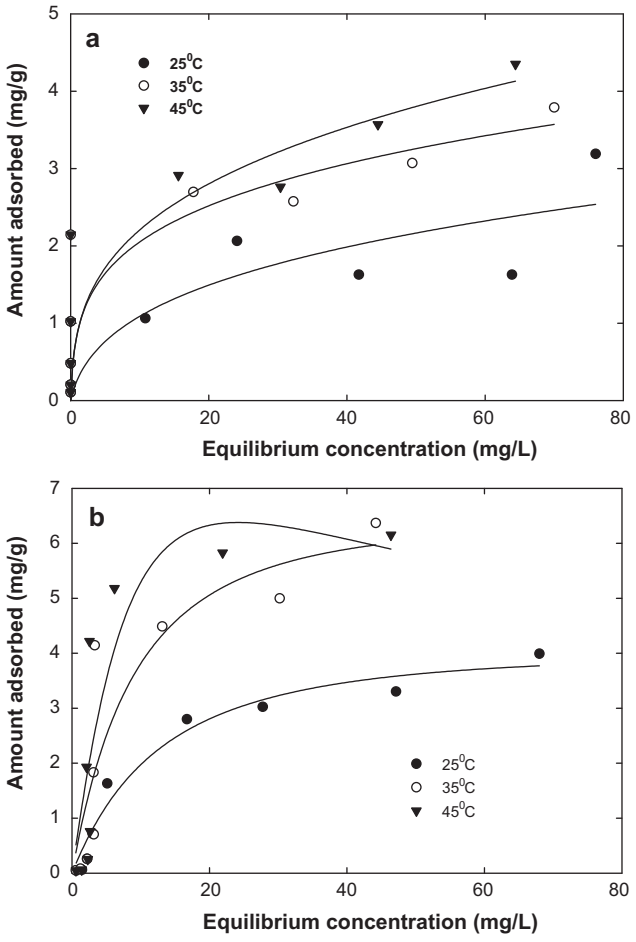

Fig. 11. Redlich–Peterson adsorption isotherms of chromium by (a) oak wood and (b) oak bark chars at different temperatures [pH 2.0, adsorbent concentration of 10 g/L]. Solid lines represent the data fitted by the Redlich–Peterson isotherm model.

on bio-chars is occurring by a combined Freundlich–Langmuir model or Sips model. In other words, adsorption is diffusion controlled at low chromium concentrations while monomolecular adsorption with a saturation value takes place at high chromium concentrations. Similar observations were reported by Muntean et al. for the adsorption of dye in wood fibers [59].

7. Swelling behavior of bio-chars

The monolayer adsorption capacities of both the chars as calculated using Langmuir adsorption isotherm model are given in Table 7. The adsorption capacities of bio-chars vis-a-vis other adsorbents are complied in Table 8. The surface area of oak wood and oak bark chars determined by nitrogen BET measurements on dry samples is very small (1–3 $m^2\ g^{-1}$) versus commercial activated carbons (~1000 $m^2\ g^{-1}$). Specifically, the bio-chars adsorb far more chromium per unit of surface area then activated carbons (Table 8). This higher Cr(VI) removal per unit surface area by the chars can be partially explained by considering the swelling of bio-chars in water. We demonstrated these chars swell in water, opening up already existing pores or adsorption sites that are closed when dry. This provides more internal surface for adsorption. Another effect is water [and Cr(VI)] diffusion into the solid walls of the chars, which contain 8–12% oxygen. This swells some of the solid structures, transporting Cr(VI) into the walls where it contacts more potential adsorption sites.

The dry weight of as-received char samples was recorded. Then char samples were immersed into water and keep immersed for the length of time that corresponds to our longer sorption experiments i.e. 48 h. Then these char samples were removed by filtration on a preweighed filter and all the surface water was removed using suction filtration. Next, the weight of the char was recorded at regular intervals to obtain weight loss as a function of time as shown in Fig. 15. It is clear that both wood and bark chars lose weight due to internal water evaporation with time. This internal water can be present in both pores and in swollen solid regions where it had diffused during immersion.

It is very clear that porosity exists in the char when submerged that was not available to gas adsorption when the char was dry. The chars' low density (it does not sink) and slow water weight loss by evaporation with time both show that the char is porous.

Proof was obtained that the surface area of the char, when submerged in water for a period, is larger than that when surface area was measured by gas adsorption on a dry sample. The weight loss (Fig. 15) due to internal water removal was about 0.19–0.20 g/g char. Thus, this water occupied about 0.19–0.20 cc/g of char. Other swelling studies revealed water volumes of 0.4 or more cc/g of char taken up by some samples. This volume must have occurred by some diffusion into pore walls and expansion of internal pore structure. This swelling is in contrast to the behavior of activated carbon. The char has ~8–12 wt.% oxygen in its structure versus carbon (~3 wt.%) [60], so it is much more polar than carbon. Secondly, during fast pyrolytic decomposition, gases and steam rapidly generated inside the wood or bark particles are "exploded" outward. As these escape from the pyrolyzing/decomposing wood or bark particles, porosity is gener-

Table 8
Comparative evaluation of Langmuir adsorption capacities of bio-chars vis-à-vis activated carbons other adsorbents for chromium removal.

Adsorbents	Type of water	pH	Temp. (°C)	Concentration range (mg/L)	Surface area (m^2/g)	Adsorption capacity (mg/g)	Adsorption capacity (mg/m^2)	References
Oak wood char	Aqueous solution	2.0	25	1–100	2.73	3.03	1.11	Present study
		2.0	35		2.73	4.08	1.50	
		2.0	45		2.73	4.93	1.80	
Oak bark char		2.0	25		1.88	4.61	2.45	
		2.0	35		1.88	7.43	3.95	
		2.0	45		1.88	7.51	4.00	
Tamarind hull activated carbon algae bloom residue derived activated carbon	Aqueous solution	2.0	30	50–150	431	85.91	0.20	[61]
Activated slog	Aqueous solution	1.0	30	1–100	107	1.41	0.13	[62]
Activated carbon, FAC	Aqueous solution	2.0	10	1–100	343.0	16.0	0.47	[2]
Activated carbon, SAC		2.0	10		378.0	1.4	0.004	
Activated carbon, ATFAC		2.0	10		512.0	1.1	0.002	
Activated carbon, ATSAC		2.0	10		380.0	1.6	0.004	
Activated carbon fabric cloth		2.0	10		1565.0	116.9	0.075	
Activated carbon, FAC		2.0	25		343.0	21.8	0.064	
Activated carbon, SAC		2.0	25		378.0	9.5	0.025	
Activated carbon, ATFAC		2.0	25		512.0	10	0.020	
Activated carbon, ATSAC		2.0	25		380.0	11.5	0.030	
Activated carbon fabric cloth		2.0	25		1565.0	96.3	0.062	
Activated carbon, FAC		2.0	40		343.0	24.1	0.070	
Activated carbon, SAC		2.0	40		378.0	32.6	0.086	
Activated carbon, ATFAC		2.0	40		512.0	15.6	0.030	
Activated carbon, ATSAC		2.0	40		380.0	16.4	0.043	
Activated carbon fabric cloth		2.0	40		1565.0	42.1	0.027	
As received coconut shell charcoal	Aqueous solution	6.0	25	5–25	5–10	2.2	~(0.220–1.1)	[63]
Coconut shell charcoal coated with chitosan		6.0	25			3.7		
Coconut shell charcoal Ox$$idized with sulfuric acid		6.0	25			4.1		
Coconut shell charcoal oxidized with sulfuric acid and coated with chitosan		6.0	25			9		
Coconut shell charcoal oxidized with nitric acid		6.0	25			11		
As received commercial activated carbon		6.0	25		900–1100	4.7	0.004–0.009	
Commercial activated carbon oxidized with sulfuric acid		6.0	25			8.9		
Commercial activated carbon oxidized with nitric acid		6.0	25			10.4		
Irish Sphagnum peat	Aqueous solution	2.5	25	100.00	>200	35.5	0.178	[64]
		2.0	25			43.9	0.220	
Composite chitosan	Aqueous solution	4.0	25	5000.0	105.2	153.8	1.462	[65]
Sawdust	Aqueous solution	2.0	25	1000.0	37.6	39.7	1.06	[66]
Sugar beet pulp				500.0	16.5	17.4	1.055	
Sugarcane bagasse				500.0	12.7	13.4	1.055	
Maiz cob				300.0	13.07	13.8	1.056	
Pistachio hull powder (PHP)	Wastewater	2.0	25	50–500	1.04	116.3	111.8	[67]

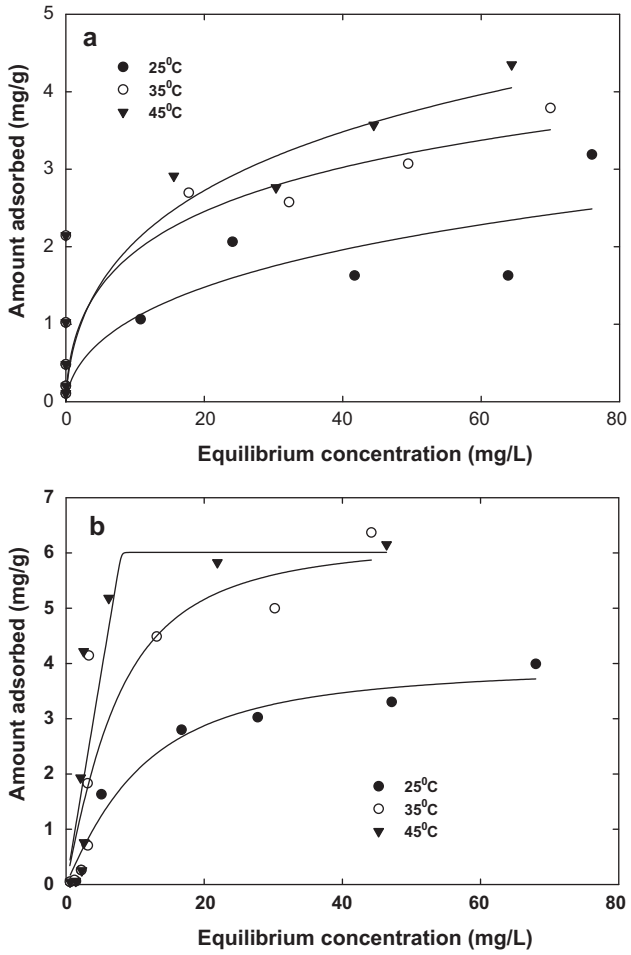

Fig. 12. Toth adsorption isotherms of hexavalent chromium by (a) oak wood and (b) oak bark chars at different temperatures [pH 2.0, adsorbent concentration of 10 g/L]. Solid lines represent the data fitted by the Toth isotherm model.

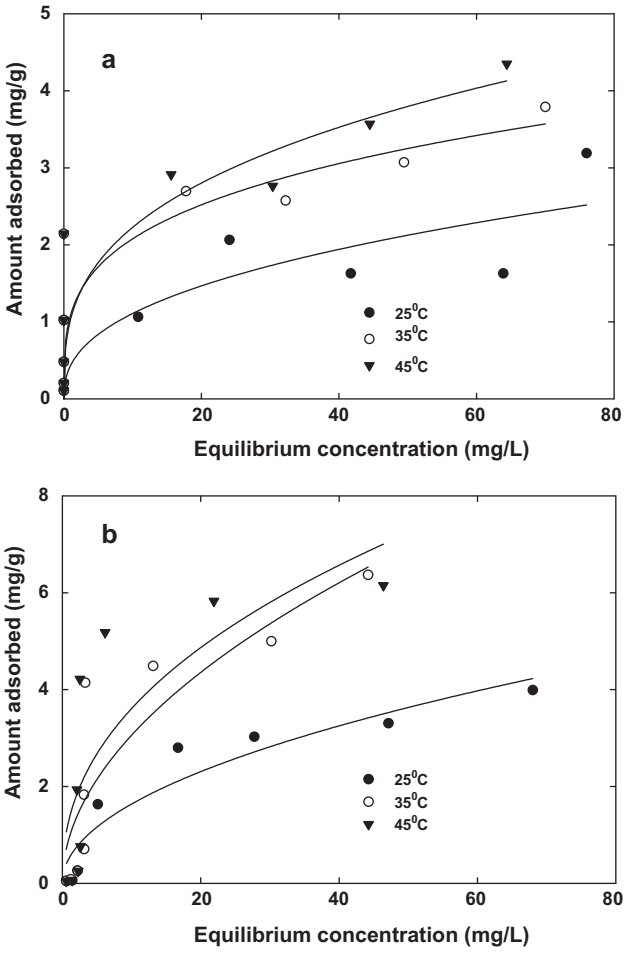

Fig. 13. Radke and Prausnitz adsorption isotherms of chromium by (a) oak wood and (b) oak bark chars at different temperatures [pH 2.0, adsorbent concentration of 10 g/L]. Solid lines represent the data fitted by the Radke and Prausnitz isotherm model.

ated by which gases escape. These internal pore networks partially collapse, melt-close during pyrolysis or close on cooling. Therefore, gas adsorption will measure a surface area that is different than the total surface that is available in water swollen samples. It is the water swollen char that is adsorbing the chromium. In contrast to these chars, activated carbon has high amounts of oxygenated functions on its pore surfaces but not within the carbon solid walls structures.

Micro or ultra micropores may exist (Table 1) in the char solids through which gases exited to the larger pores. Some cannot be seen at the SEM resolution (Figs. 1 and 2). They have likely closed and only open when water is imbibed. Water either opens such pores or, even more likely, DIFFUSES INTO these walls (carrying chromium ions). Thus, much of the solid (seen on micrographs) may be able to adsorb chromium within these wall structures. This cannot happen with activated carbon because its walls are almost pure, solid, hydrophobic carbon below the pore wall surfaces so water cannot diffuse into that solid. Thus, the chromium does not ONLY adsorb on the surfaces of the visible pores by SEM, but ALSO is adsorbed inside these cell walls as water diffuses into at least portions of these walls.

8. Application of these bio-chars to treat surface water samples

The challenge in batch adsorption studies is that actual water/wastewater systems contain a complex multi-solute mixture of ions. When the adsorption of a target species is of interest, the effect of competition for adsorption sites with other aqueous metals present in the matrix affects the overall sorption efficacy of the adsorbent.

To study the effect of possible competition, surface water sample was collected from the Lutfullapur, Navada, Loni, District Ghaziabad, India. The physicochemical characteristics of this water sample are given in Table 9. An additional ~5.0 mg/L of hexavalent chromium was spiked into this surface water sample. Oak bark and oak wood chars were then utilized to remove hexavalent chromium from this surface water under the optimum conditions (obtained by batch sorption studies). The pH of the simulated water was adjusted to 2.0 before applying bio-chars. A predetermined amount (5 g/L) of bio-char was added to each sample. After 48 h of equilibration, the samples were filtered using Whatman No. 1 paper. Then the hexavalent chromium concentrations were measured by UV–visible spectroscopy at 540 nm after color development by adding diphenyl carbazide. It is clear from Table 9 that the final Cr(VI) concentrations were reduced to only 1/6 in case of oak bark and 1/2 in case of oak wood of their original values. Thus, Cr(VI) removal was higher with oak bark char versus oak wood char. This agreed with the batch experiments conducted with synthetic samples. Furthermore, the presence of solids and interfering ions present in surface water caused slight reductions in the chars' sorption capacities. Thus, the char samples can be applied to chromium remediation from contaminated surface and/or ground water.

Table 9
Chromium(VI) remediation of a contaminated surface water[a] using oak wood and oak bark chars (adsorbent dose 5 g/L; equilibrium time 48 h; pH 2.0; temperature 25 °C; volume of the water sample taken 50 mL).

Parameters	Values without any pH adjustment	Values when pH adjustment was done (initial pH 8.33 which is adjusted to pH-2)	Values after treatment with oak wood char	Values after treatment with oak bark char
pH	8.55	1.99	2.02	2.43
ORP (mV)	−43.8	+293.4	+288.8	+270.6
Conductivity (μS/cm)	1598.0	7370	6940	2367.0
TDS (mg/L)	1068	3602	2235.0	1975.0
Na^+ (mg/L)	321	340	343	363
K^+ (mg/L)	149	144	146	161
Ca^{2+} (mg/L)	138	28	37.4	60.0
Ba^{2+} (mg/L)	144	86.5	96.7	120.0
Li^+ (mg/L)	0.5	0.5	0.5	0.4
Cr^{6+} (mg/L)	ND	4.467	2.054	0.784

[a] Surface water sample was collected from Lutfullapur, Navada, Loni, District Ghaziabad, India and an additional ~5.0 mg/L of hexavalent chromium was spiked into this surface water sample.

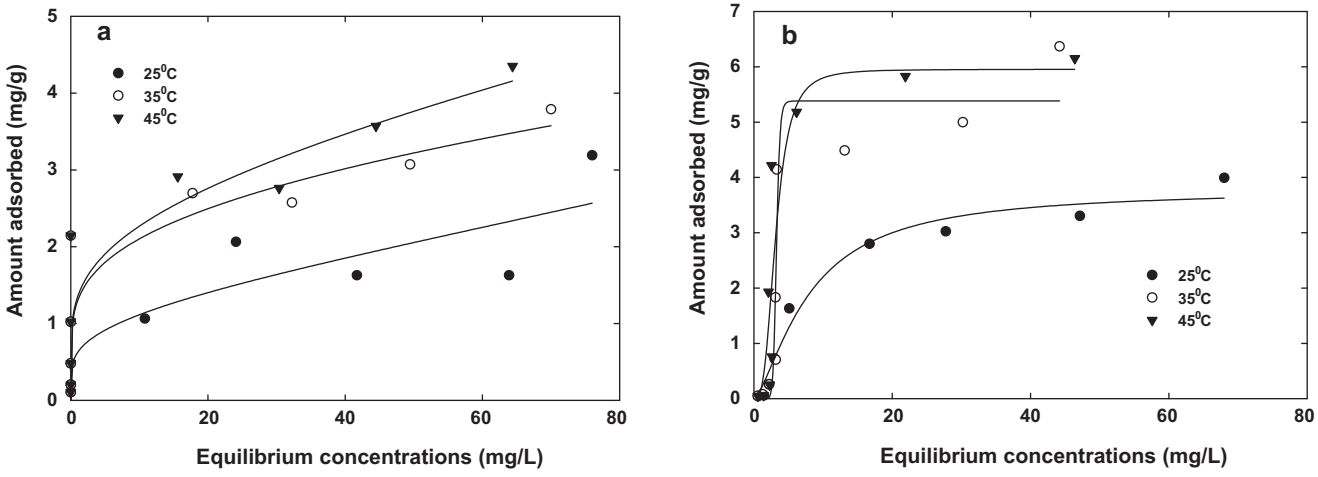

Fig. 14. Sips adsorption isotherms of chromium by (a) oak wood and (b) oak bark chars at different temperatures [pH 2.0, adsorbent concentration of 10 g/L]. Solid lines represent the data fitted by the Sips isotherm model.

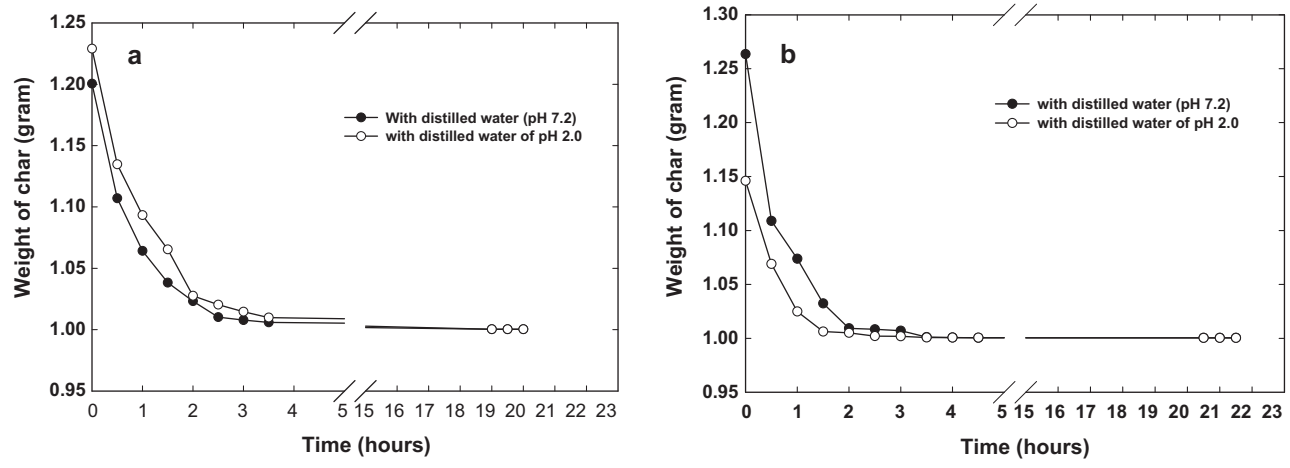

Fig. 15. Swelling behavior measured by loss of imbibed water weight by evaporation (a) oak wood and (b) oak bark at 25 °C in water at pH 7.2 and pH 2.0 after 48 h of immersion.

9. Conclusions

The chars produced by pyrolysis of oak wood and oak bark at 400 and 450 °C in an auger-fed reactor during bio-oil production were characterized and used successfully without activation for the hexavalent chromium remediation from water. The chromium removal was higher with oak bark char versus oak wood char. The chromium adsorption on oak wood and oak bark chars at different temperatures followed the order: $Q^0_{\text{oak bark}}$, 45 °C > $Q^0_{\text{oak bark}}$, 35 °C > $Q^0_{\text{oak wood}}$, 45 °C > $Q^0_{\text{oak bark}}$, 25 °C > $Q^0_{\text{oak wood}}$, 35 °C > $Q^0_{\text{oak wood}}$, 25 °C.
Chromium sorption capacities of bio-chars are comparable to

the activated carbons and other materials reported for chromium decontamination (Table 8). Chromium adsorption increased with increase in temperature indicating the process is endothermic. The rate of chromium adsorption was explained by a pseudo-second-order kinetic model. The pseudo-second order model is based on the assumption that the rate-limiting step is a chemical sorption between the adsorbate and adsorbent.

The Sips or Langmuir–Freundlich adsorption isotherm model best fits the experimental data, giving the highest regression (R^2) coefficients. This shows that chromium adsorption on bio-chars occurs by a combined Freundlich and Langmuir model, i.e. diffusion controlled adsorption predominates at low chromium concentration, and monomolecular adsorption proceeds at high chromium concentrations. The oak wood and oak bark char samples were applied successfully to remediate hexavalent chromium from contaminated surface water. Solids and other interfering ions did not reduce the ability of bio-chars to remove and led to no or only nominal reduction of sorption capacity.

The surface area of tested oak wood and oak bark chars is very small (1–3 $m^2\,g^{-1}$) versus the very high value for commercial activated carbons (1000 $m^2\,g^{-1}$). Specifically, the biochars adsorb far more Cr(VI) per unit of surface area then activated carbons (Table 8). Water was found to cause swelling of the char that created more internal char/water contact. This feature likely leads to greater adsorption capacity. The surface area of these chars could, in near future be further increased by steam activation and/or chemical treatments to improve their removal efficacy. Byproduct chars from bio-oil production might be used as plentiful inexpensive adsorbents for water treatment at a value above their pure fuel value.

Further studies of such chars, both untreated and after activation, seem warranted as part of the efforts to generate byproduct value from biorefineries.

Acknowledgements

Financial support of this work at Jawaharlal Nehru University, New Delhi, India was provided by University Grant Commission (PAC/SES/DM/UGC/0210113-491)) New Delhi, Department of Science and Technology (DST-PURSE) New Delhi and Jawaharlal Nehru University (Capacity Build-up funds). Financial support at Mississippi State University was provided by USDA (Grant no. 68-3475-4-142).

References

[1] D. Mohan, C.U. Pittman Jr., Activated carbons and low cost adsorbents for remediation of tri- and hexavalent chromium from water, Journal of Hazardous Materials 137 (2006) 762–811.
[2] D. Mohan, K.P. Singh, V.K. Singh, Removal of hexavalent chromium from aqueous solution using low-cost activated carbons derived from agricultural waste materials and activated carbon fabric cloth, Industrial and Engineering Chemistry Research 44 (2005) 1027–1042.
[3] D. Mohan, K.P. Singh, V.K. Singh, Trivalent chromium removal from wastewater using low cost activated carbon derived from agricultural waste material and activated carbon fabric cloth, Journal of Hazardous Materials 135 (2006) 280–295.
[4] L.R. Radovic, C. Moreno-Castilla, J. Rivera-Utrilla, Carbon materials as adsorbents in aqueous solutions, in: L.R. Radovic (Ed.), Chemistry and Physics of Carbon, Marcel Dekker Inc., New York, 2000.
[5] R.J. Irwin, M.V.N. Mouwerik, L. Stevens, M.D. Seese, W. Basham, Environmental Contaminants Encyclopedia Chromium(VI) (Hexavalent Chromium) Entry, National Park Service Water Resources Divisions, Fort Collins, CO, 1971.
[6] D.E. Kimbrough, Y. Cohen, A.M. Winer, L. Creelman, C.A. Mabuni, Critical assessment of chromium in the environment, Critical Reviews in Environment Science and Technology 29 (1999) 1–46.
[7] R.J. Lancashire, http://www.chem.uwimona.edu.jm/courses/chromium.html.
[8] R.K. Singh, B. Sengupta, R. Bali, B.P. Shukla, V.V.S. Gurunadharao, R. Srivatstava, Identification and mapping of chromium (VI) plume in groundwater for remediation: a case study at Kanpur, Uttar Pradesh, Journal of the Geological Society of India 74 (2009) 49–57.
[9] US EPA/625/R-00/005, In-situ treatment of soil and groundwater contaminated with chromium, Technical Resources Guide, United States Environmental Protection Agency.
[10] Bureau of Indian Standards IS 10500, 1991, BIS 2003, New Delhi, India.
[11] J.W. Paterson, Wastewater Treatment Technology, Ann Arbour Science, Michigan, 1975.
[12] A.K. Yadav, N. Kumar, T.R. Sreekrishnan, S. Satya, N.R. Bishnoi, Removal of chromium and nickel from aqueous solution in constructed wetland: mass balance, adsorption–desorption and FTIR study, Chemical Engineering Journal 160 (2010) 122–128.
[13] R.T. Bachmann, D. Wiemken, A.B. Tengkiat, M. Wilichowski, Feasibility study on the recovery of hexavalent chromium from a simulated electroplating effluent using Alamine 336 and refined palm oil, Separation and Purification Technology 75 (2010) 303–309.
[14] S. Edebali, E. Pehlivan, Evaluation of Amberlite IRA96 and Dowex 1×8 ion-exchange resins for the removal of Cr(VI) from aqueous solution, Chemical Engineering Journal 161 (2010) 161–166.
[15] X. Ren, C. Zhao, S. Du, T. Wang, Z. Luan, J. Wang, D. Hou, Fabrication of asymmetric poly (m-phenylene isophthalamide) nanofiltration membrane for chromium(VI) removal, Journal of Environmental Sciences 22 (2010) 1335–1341.
[16] G. Ghosh, P.K. Bhattacharya, Hexavalent chromium ion removal through micellar enhanced ultrafiltration, Chemical Engineering Journal 119 (2006) 45–53.
[17] Z. Song, C.J. Williams, R.G.J. Edyvean, Sedimentation of tannery wastewater, Water Research 34 (2000) 2171–2176.
[18] V.K. Gupta, S.K. Srivastava, D. Mohan, Design parameters for fixed bed reactors of activated carbon developed from fertilizer waste for the removal of some heavy metal ions, Waste Management 17 (1997) 517–522.
[19] V.K. Gupta, M. Gupta, S. Sharma, Process development for the removal of lead and chromium from aqueous solutions using red mud-an aluminium industry waste, Water Research 35 (2001) 1125–1134.
[20] J. Lakatos, S.D. Brown, C.E. Snape, Coals as sorbents for the removal and reduction of hexavalent chromium from aqueous waste streams, Fuel 81 (2002) 691–698.
[21] A. Idris, N. Hassan, N.S.M. Ismail, E. Misran, N.M. Yusof, A.-F. Ngomsik, A. Bee, Photocatalytic magnetic separable beads for chromium(VI) reduction, Water Research 44 (2010) 1683–1688.
[22] T. Liu, L. Zhao, D. Sun, X. Tan, Entrapment of nanoscale zero-valent iron in chitosan beads for hexavalent chromium removal from wastewater, Journal of Hazardous Materials 184 (2010) 724–730.
[23] P. Yuan, D. Liu, M. Fan, D. Yang, R. Zhu, F. Ge, J. Zhu, H. He, Removal of hexavalent chromium [Cr(VI)] from aqueous solutions by the diatomite-supported/unsupported magnetite nanoparticles, Journal of Hazardous Materials 173 (2010) 614–621.
[24] V.K. Gupta, A. Rastogi, A. Nayak, Adsorption studies on the removal of hexavalent chromium from aqueous solution using a low cost fertilizer industry waste material, Journal of Colloid and Interface Science 342 (2010) 135–141.
[25] S. Sharma, A. Malik, S. Satya, Application of response surface methodology (RSM) for optimization of nutrient supplementation for Cr(VI) removal by *Aspergillus lentulus* AML05, Journal of Hazardous Materials 164 (2009) 1198–1204.
[26] J. Wu, H. Zhang, P.-J. He, Q. Yao, L.-M. Shao, Cr(VI) removal from aqueous solution by dried activated sludge biomass, Journal of Hazardous Materials 176 (2010) 697–703.
[27] B. Saha, C. Orvig, Biosorbents for hexavalent chromium elimination from industrial and municipal effluents, Coordination Chemistry Reviews 254 (2010) 2959–2972.
[28] S. Babel, T.A. Kurniawan, Low cost adsorbents for heavy metals uptake from contaminated water: a review, Journal of Hazardous Materials B 97 (2003).
[29] S.J.T. Pollard, G.D. Fowler, C.J. Sollars, R. Perry, Low cost adsorbents for waste and wastewater treatment: a review, Science of the Total Environment 116 (1992) 31–52.
[30] D. Mohan, C.U. Pittman Jr., P.H. Steele, Single, binary and multi-component adsorption of copper and cadmium from aqueous solutions on Kraft lignin-a biosorbent, Journal of Colloid and Interface Science 297 (2006) 489–504.
[31] D. Mohan, S. Chander, Removal and recovery of metal ions from acid mine drainage using lignite—a low cost sorbent, Journal of Hazardous Materials 137 (2006) 1545–1553.
[32] D. Mohan, K.P. Singh, V.K. Singh, Wastewater treatment using low cost activated carbons derived from agricultural byproducts—a case study, Journal of Hazardous Materials 152 (2008) 1045–1053.
[33] D. Mohan, K.P. Singh, S. Sinha, D. Gosh, Removal of pyridine derivatives from aqueous solution by activated carbons developed from agricultural waste materials, Carbon 43 (2005) 1680–1693.
[34] D. Mohan, K.P. Singh, S. Sinha, D. Gosh, Removal of pyridine from aqueous solution using low cost activated carbons derived from agricultural waste materials, Carbon 42 (2004) 2409–2421.
[35] M. Fan, W. Marshall, D. Daugaard, R.C. Brown, Steam activation of chars produced from oat hulls and corn stover, Bioresource Technology 93 (2004) 103–107.
[36] W. Zheng, M. Guo, T. Chow, D.N. Bennett, N. Rajagopalan, Sorption properties of greenwaste biochar for two triazine pesticides, Journal of Hazardous Materials 181 (2010) 121–126.
[37] D. Mohan, C.U. Pittman Jr., M. Bricka, F. Smith, B. Yancey, J. Mohammad, P.H. Steele, M.F. Alexandre-Franco, V. Gómez-Serrano, H. Gong, Sorption of arsenic,

cadmium, and lead by chars produced from fast pyrolysis of wood and bark during bio-oil production, Journal of Colloid and Interface Science 310 (2007) 57–73.
[38] S Brunauer, P.H. Emmett, E. Teller, Adsorption of gases in multimolecular layers, Journal of the American Chemical Society 60 (1938) 309–319.
[39] M.M. Dubinin, Progress in Surface and Membrane Science, Academic Press, New York/London, 1975.
[40] M.M. Dubinin, G.M. Plavnik, Microporous structures of carbonaceous adsorbents, Carbon 6 (1968) 183–192.
[41] G. McKay, Use of Adsorbents for the Removal of Pollutants from Wastewaters, CRC Press, Boca Raton, FL, 1995.
[42] A.I. Vogel, A Textbook of Quantitative Chemical Analysis, ELBS Publication, London, 1989.
[43] V. Gómez-Serrano, C.M. González-García, M.L. González-Martín, Nitrogen adsorption isotherms on carbonaceous materials. Comparison of BET and Langmuir surface areas, Powder Technology 116 (2001) 103–108.
[44] J.E. Amonette, S. Joseph, Characteristics of biochar: microchemical properties, in: J. Lehmann, S. Joseph (Eds.), Biochar for Environmental Management, Earthscan, UK, London, 2009, pp. 34–52.
[45] V.K. Gupta, D. Mohan, S. Sharma, K.T. Park, Removal of chromium(VI) from electroplating industry wastewater using bagasse fly ash—a sugar industry waste material, The Environmentalist 19 (1999) 129–136.
[46] S.K. Srivastava, V.K. Gupta, D. Mohan, Kinetic parameters for the removal of lead and chromium from wastewater using activated carbon developed from fertilizer waste material, Environmental Modeling and Assessment 1 (1997) 281–290.
[47] D. Park, Y.-S. Yun, J.H. Jo, J.M. Park, Mechanism of hexavalent chromium removal by dead fungal biomass of *Aspergillus niger*, Water Research 39 (2005) 533.
[48] S. Lagergren, der Sogenannten adsorption geloster Stoffe, Kungliga Svenska Vetenska Psalka de Miens Handlingar 24 (1898).
[49] Y.-S. Ho, D.A.J. Wase, C.F. Forster, Kinetic studies of competitive heavy metal adsorption, Environmental Technology 17 (1996) 71.
[50] Y.S. Ho, G. McKay, Pseudo-second order model for sorption processes, Process Biochemistry 34 (1999) 451.
[51] V.C. Taty-Costodes, H. Fauduet, C. Porte, A. Delacroix, Removal of Cd(II) and Pb(II) ions from aqueous solutions, by adsorption onto sawdust of *Pinus sylvestris*, Journal of Hazardous Materials 105 (2003) 121–142.
[52] H.M.F Freundlich, Over the adsorption in solution, Journal of Physical Chemistry 57 (1906) 385–470.
[53] I. Langmuir, The adsorption of gases on plane surface of glass, mica and platinum, Journal of American Chemical Society 40 (1916) 1361–1368.
[54] K.R. Hall, L.C. Eagletow, A. Acrivers, T. Vermenlem, Pore and solid kinetics in fixed-bed adsorption under constand pattern condition, Industrial Engineering and Chemistry Fundamentals 5 (1966) 212–218.
[55] O. Redlich, D.L. Peterson, A useful adsorption isotherm, Journal of Physical Chemistry 63 (1959) 1024.
[56] S.J. Allen, G. Mckay, J.F. Porter, Adsorption isotherm models for basic dye adsorption by peat in single and binary component systems, Journal of Colloid and Interface Science 280 (2004) 322–333.
[57] C.J. Radke, J.M. Prausnitz, Adsorption of organic solutes from dilute aqueous solution on activated carbon, Industrial and Engineering Chemistry Fundamental 11 (1972) 445–451.
[58] R. Ship, Combined form of Langmuir and Freundlich equations, Journal of Chemical Physics 16 (1948) 490–495.
[59] S.G. Muntean, G. Simu, P. Sfarloaga, C. Bologa, Study of a trisazo direct dye adsorption on wood fibre using a comparison of different adsorption isotherms, Revista de Chimie 61 (2010).
[60] R. Pardo-Botello, C. Fernández-González, E. Pinilla-Gil, E.M. Cuerda-Correa, V. Gómez-Serrano, Adsorption kinetics of zinc in multicomponent ionic systems, Journal of Colloid and Interface Science 277 (2004) 292–298.
[61] A. Verma, S. Chakraborty, J.K. Basu, Adsorption study of hexavalent chromium using tamarind-hull based adsorbents, Separation and Purification Technology 50 (2006) 336–341.
[62] S.K. Srivastava, V.K. Gupta, D. Mohan, Removal of lead and chromium by activated slag-a blast furnace waste, Journal of Environment Engineering (ASCE) 123 (1997) 461–468.
[63] S. Babel, T.A. Kurniawan, Cr(VI) removal from synthetic wastewater using coconut shell charcoal and commercial activated carbon modified with oxidizing agents and/or chitosan, Chemosphere 54 (2004) 951–967.
[64] D.C. Sharma, C.F. Forster, Continuous adsorption and desorption of chromium ions by sphagnum moss peat, Process Biochemistry 30 (1995) 293–298.
[65] V.M. Boddu, K. Abburi, J.L. Talbott, E.D. Smith, Removal of hexavalent chromium from wastewater using a new composite chitosan biosorbent, Environmental Science and Technology 37 (2003) 4449–4456.
[66] D.C. Sharma, C.F. Forster, A preliminary examination into the adsorption of hexavalent chromium using low-cost adsorbents, Bioresource Technology 47 (1994) 257–264.
[67] G. Moussavi, B. Barikbin, Biosorption of chromium(VI) from industrial wastewater onto pistachio hull waste biomass, Chemical Engineering Journal 162 (2010) 893–900.